Available online at www.sciencedirect.com

ScienceDirect

Procedia CIRP 108 (2022) 704–709

www.elsevier.com/locate/procedia

6th CIRP Conference on Surface Integrity

Areal surface texture and tool wear analysis from machining during powder bed fusion

Kossi Loic M. Avegnon[a,d], David C. Schmitter[a], Sandra Meisman[a], Haitham Hadidi[c], Benoit Vieille[b], Michael P. Sealy[a,b,d]*

[a]University of Nebraska-Lincoln, Mechanical and Materials Engineering, 1400 R Street, Lincoln, NE 68588, USA
[b]National Institute of Applied Sciences (INSA), Group of Materials Physics, 685 Av. de l'Université, 76800 Saint-Étienne-du-Rouvray, France
[c]Jazan University, Department of Mechanical Engineering, Al Maarefah Rd, Ash Shati, Jazan 82817, Saudi Arabia
[d]Purdue University, School of Mechanical Engineering, 610 Purdue Mall, West Lafayette, IN 47907, USA

* Corresponding author. Tel.: +1 (765) 496-7569; *E-mail address:* msealy@purdue.edu

Abstract

Coupling additive manufacturing with milling changes the interaction between the cutting tool and workpiece. The resulting effect on tool wear and surface integrity is poorly understood. Maraging steel printed via powder bed fusion was peripherally milled in the presence of un-melted metallic powder surrounding the printed part. Areal surface parameters, microhardness, and tool wear were analyzed. Results showed that milling within powder decreased surface roughness and introduced a weak orthogonal texture between the feed marks and printed layers. Milling without powder caused a more pronounced inclined texture. Milling within powder accelerated flank wear while milling without powder accelerated crater wear.

Keywords: hybrid AM; milling; surface texture; tool wear

1. Introduction

Coupling additive manufacturing with milling has the advantage of reducing the lead time of components by achieving the desired surface roughness in one hybrid build envelope. The problem is that cutting in powder changes the cutting mechanics and interaction between the cutting tool and workpiece. The resulting effect on tool wear, surface roughness, and mechanical properties is still poorly understood.

The relatively high surface roughness obtained after powder bed fusion often requires post-process milling to improve the surface quality. The surface integrity of additively manufactured components affects the performance in a service environment. Apart from increasing production time and cost, a post-process milling operation is often impractical and may require specialized tooling. To alleviate the need for special tooling and additional processing, hybrid additive manufacturing systems were developed to print and mill in a sequential manner to achieve the desired surface finish in one machine platform. Commercial machine platforms have combined milling with directed energy deposition systems (*e.g.*, Optomec, Mazak, DMG Mori) and powder bed fusion systems (*e.g.*, Matsuura and Sodick) to achieve a surface roughness (Sa) less than 0.8 µm [1, 2]. Finished machined surfaces are possible directly from the build chamber. The first known study on combined in-envelope powder bed fusion and milling was in 2006 by Matsushita Electric Works, Ltd. (Panasonic Electric Works outside Japan) and Kanazawa University to manufacture a

10.1016/j.procir.2022.03.109

mold with deep ribs using maraging steel [3]. It was observed that the hybrid process shortened the lead time by 50% compared to conventional machining processes. Milling with the existence of fine un-melted metallic powder surrounding the sintered part (milling within powder) increased the tool flank temperature and the specific energy of the milling process by 7% and 14%, respectively [4]. The most significant parameter during the in-situ milling was the radial depth of cut [2]. The ball end mill using while milling in-powder was subjected to non-uniform wear, chipping, and adhesion as the dominant wear mechanisms [5, 6]. The material used in these previous studies was maraging steel due to its high hardness and good machinability [3, 7, 8]. This technology opens the possibility to tailor the manufacturing process for specific components because of the adjustment on the surface and sub-surface during the milling [9].

The system employed in this study was a Matsuura Lumex Avance-25 that combines powder bed fusion with high-speed micro-milling (Fig. 1a). The aim of this research was to investigate the influence of unmelted powder on the cutting mechanics and resulting surface topography when a milling tool is plunged into powder on a hybrid powder bed fusion system. The presence of unmelted powder surrounding the workpiece is expected to affect the tool-workpiece interaction. Existing literature on in-powder milling versus traditional out-of-powder milling does not fully characterize spatial parameters. Analyzing the surface roughness alone is insufficient for understanding the complexities of cutting in powder-based medium. Thus, there is a need to characterize the surface texture and feature wavelength using an autocorrelation function. More specifically, the objective of this study was to characterize the surface of maraging steel using spatial parameters to understand how the tool engaged with workpiece when abrasive powder particles disrupt the cutting process. The results were compared to a control condition with out-of-powder milling using identical cutting conditions within the same build chamber.

Nomenclature

ACF	autocorrelation function
HV	Vicker's microhardness
Sa	arithmetic height
Sal	auto-correlation length
Sku	kurtosis
Sp	maximum peak height
Sq	root mean square height
Ssk	skewness
Std	texture direction
Str	texture aspect ratio
Sv	maximum pit height
Sz	maximum height

2. Materials and Methods

2.1 Powder bed fusion

Samples were manufactured with Matsuura Maraging Steel powder using a fourth generation Matsuura Lumex Avance-25 hybrid system. The powder size was 29 ± 10 µm (Fig. 1b). The layer thickness, laser power, and scanning speed were 50 µm, 280 W, and 700 mm/s, respectively. The scanning speed of the contour (vector) was 1400 mm/s. An extra 0.5 mm stock was added to all sides of the specimen to achieve a final dimension of (L) 80 mm × (W) 10 mm × (T) 4 mm. The build-plate was kept at 50°C throughout the print and the raster orientation was randomized using ±45° within 5 mm × 5 mm cells.

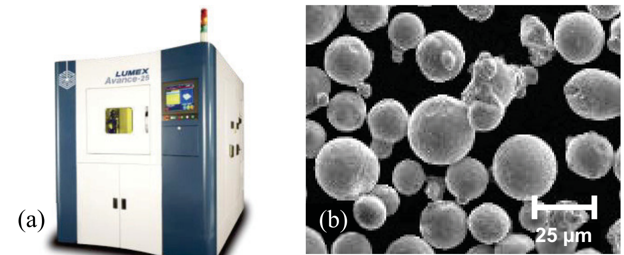

Fig. 1 (a) Matsuura Lumex Avance-25 (4th generation) hybrid powder bed fusion system and (b) Matsuura maraging steel powder.

2.2 Post-print milling

After printing, samples were milled within the build chamber with and without the presence of un-melted powder surrounding the part (Fig. 2). The milling conditions and the tool specifications are shown in Table 1. It should be noted that this investigation did not use a motion study of the milling operation from Lumex-CAM in order to simplify the analysis. Lumex-CAM defaults to multiple roughing and finishing cuttings of various size based on the geometry during the build process. Instead, one VF-HVRB 6 mm diameter cutting tool designed for high speed milling by Mitsubishi Materials was employed. The tool started at the top of the build and peripherally down-milled the sidewalls towards the build plate at step heights of 0.5 mm as a post-print machining

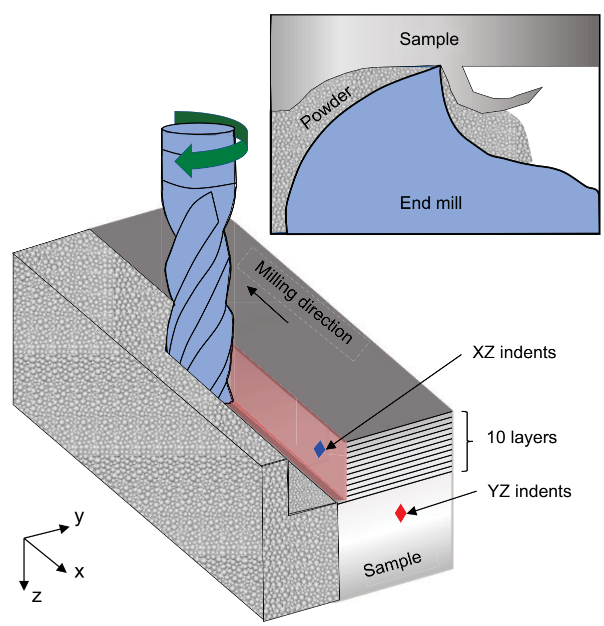

Fig. 2 Milling in powder.

operation. In this manner, the cutting tool was plunged deeper in powder than what would happen under default parameters on a Matsuura Lumex Avance-25. The total number of machining steps was 20 passes where each step encompassed ten printed layers. The surface texture and tool wear for machining in-powder was compared to a sample milled without the presence of powder using identical cutting conditions.

Table 1. Milling parameters

Cutting Process Parameters	Value
Radial depth of cut (a_e):	0.5 mm
Cutting speed (v):	39 m/min
Feed per tooth (f):	0.03 mm/tooth
Material removal rate (MRR):	4.17 mm^3/s
Milling mode:	Down milling
Tool diameter:	6 mm
No of flutes:	4
Corner radius:	0.5 mm

2.3 Areal Analysis of height and spatial parameters

Areal analysis was investigated across the milled surface using a Keyence VK-X200K 3D laser scanning confocal microscope. Scanning was done using a standard 5x lens with an XY calibration of 2.8 µm/pixel. The data was analyzed using VK Analyzer 3.4.0.1, and the profile roughness comparisons were made according to the ASTM standards ISO 25178. The data was filtered using the S-filer (100 µm) and the L-filter (500µm) before analysis. The data was not processed using the F-operator filter since the scanned area was already flat. Height and spatial parameters of the machined surfaces were analyzed in this study.

The arithmetic mean height (Sa), which is frequently employed to characterize surface roughness, quantifies the mean height of peaks and valleys of interest without regard to direction (*i.e.*, average of the absolute value of height). Other standard height parameters, such as Sp, Sv, Sq, Ssk, and Sku, are included in Table 2 for completeness. Although height parameters are a convenient metric for areal characterization, information regarding the texture motif are not captured [10]. Spatial parameters are therefore used to further describe the texture and orientation of the surface. The spatial parameters used in this study were autocorrelation length (Sal), texture aspect ratio (Str), and texture direction (Std).

The autocorrelation function (ACF) evaluates the correlation of a part of an image with respect to the whole image. The ACF is used to study periodicities on a surface when a texture motif is reproduced several times or is used to assess the isotropy of a surface. The autocorrelation length (Sal) of a surface is defined as the horizontal distance of the ACF which has the fastest decay to a specified value s of 0.2. Sal provides information about the fineness of the surface (Fig. 3). A smaller Sal value represents a surface with finer features [10]. The texture aspect ratio parameter (Str) is a numerical representation of the strength of orientation. Str < 0.3 signifies an anisotropic (directional) surface, while Str > 0.5 represents an isotropic surface [11]. The texture direction (Std) of the surface captures the primary directionality(ies) exhibited on a surface. Std is calculated by decomposing the surface into spatial frequencies from the Fourier spectrum [10]. Std is represented by the spatial frequency plotted in polar coordinates at angles corresponding to the primary texture direction(s).

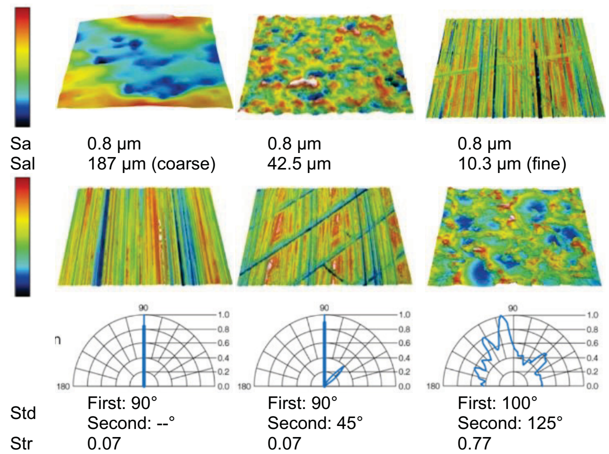

Fig. 3 Exemplary surfaces to define autocorrelation length (Sal) and texture direction (Std). Modified from [11].

3. Results and Discussion

The resulting sidewall surfaces from milling an additively manufactured block within and without powder are shown in Fig. 4. Milling in presence of powder decreased the quality of the obtained surface. When milling without powder, the vertical feed marks on the surface were less aligned (*i.e.*, more skewed) compared to milling within powder. The micro-scale differences between the two surfaces were analyzed through the arithmetic height (Sa), the auto-correlation length (Sal), and the texture direction (Std). The height and spatial parameters from milling within and without powder are provided in Tables 2 and 3.

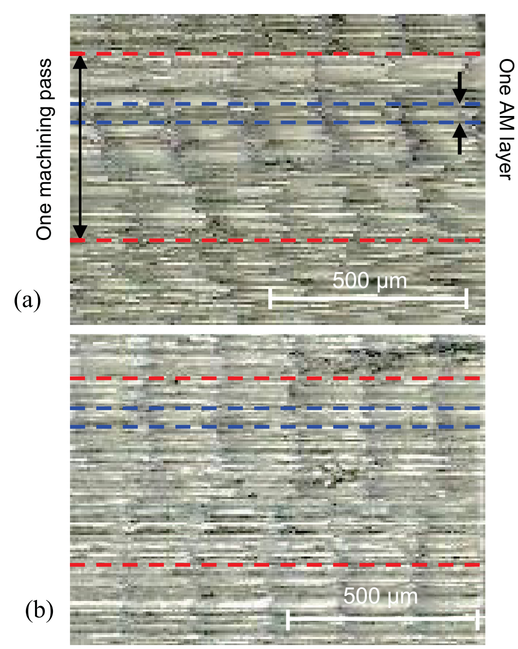

Fig. 4 Surface of maraging steel after milling on a Matsuura Lumex Avance-25 (a) without powder and (b) within powder.

Table 2 Height parameters from milling within and without powder

Height parameters	Within powder	Without powder
Sa (µm)	1.86	2.65
Sq (µm)	2.38	3.42
Sku	3.665	4.228
Sv (µm)	15.46	18.31
Ssk	-0.246	0.683
Sp (µm)	14.03	10.93
Sz (µm)	29.49	29.24

3.1 Surface roughness

The continuous presence of powder resulted in an improved surface roughness from peripheral milling. The Sa from milling within powder was 30% smoother than milling without powder. The Sa likely improved while cutting within powder because of a burnishing effect of the spherical powder particles. This is likely why the skewness (Ssk) of the surface from milling within powder was negative while the surface milled without powder was positively skewed. The powder particles acted to round off the peaks.

3.2 Spatial parameter analysis

The values of Sal were similar between milling within and without powder (approximately 44 µm). Again, this represents the fastest decay autocorrelation length. Given that the layer thickness from printing and the cutting conditions were identical, the driving feature was the machining feed marks, which were not statistically different. Cutting in powder did not affect the wavelength of these surfaces.

On the contrary, the two surfaces exhibited distinct textures (Figs. 5 and 6). The texture aspect ratio (Str) for the surface milled within powder was 0.79, which indicated the surface texture was more spatially isotropic. The surface milled without powder (Str = 0.33) exhibited more directionality, although it was relatively weak. In terms of direction, the lay (Std) of the surfaces milled within and without powder were not similar. The first angle of the Std as shown in the figure below was close to 0 or 180 degrees. This meant both surface textures were predominantly horizontal and corresponded with the 3D printed layers. The second texture direction of the feed marks between both surfaces was different. The surface milled within powder exhibited a 90-degree secondary directionality. The surface milled without powder exhibited a weaker 110-to-120-degree secondary direction.

The inclined feed marks versus vertical feeds marks may be attributed to changes in the tool workpiece interface from having powder in the flutes of the cutting tool. It may also be related to the stability and or vibration of the cut from milling within and without powder. The tendency to create irregular (inclined) feed marks and rough surface has been attributed to the high cutting forces resulting from the cutting direction and contact between tool and workpiece causing cutter vibration and hence inconsistency in the obtained feed marks as discussed by [12]. Kang *et al.* [13] also discussed the effect of cutting forces on vibration and surface characteristics. It was found that in the horizontal upward direction and vertical upward direction, which have higher linear speed of cutting than the downward direction under the same gradient, the tool axis does not vibrate as in the former case, while it does in the latter. Such a vibration of the tool axis shortens tool life in ball-end milling, when intermittently cutting because it causes chipping of the tool and flank wear caused by shocks. In this study, the powder may act in a similar role to reduce vibration or shock loading.

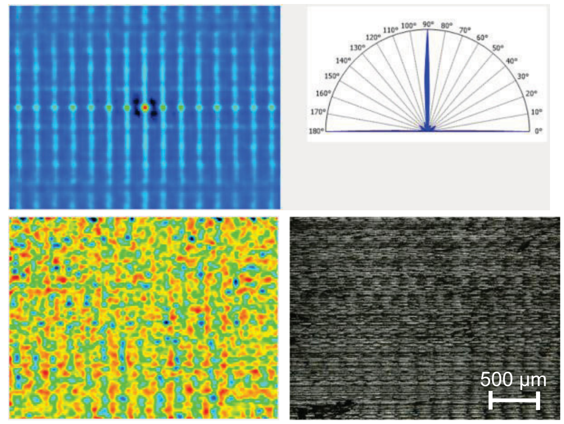

Fig. 5 Autocorrelation function at 2.5 mm from the top surface after milling within powder.

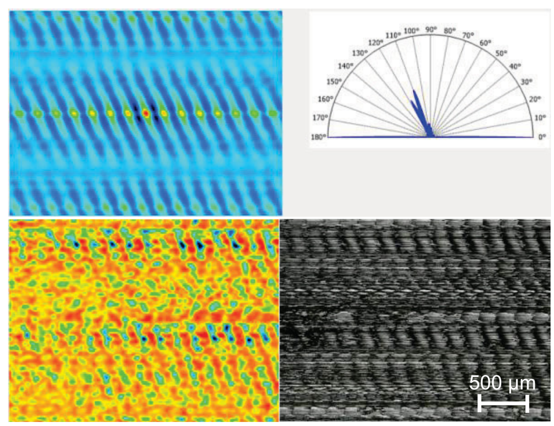

Fig. 6 Autocorrelation function at 2.5 mm from the top surface after milling without powder.

Table 3 Spatial parameters from milling within and without powder

Spatial parameters	Within powder	Without powder
Sal (µm)	43.79	44.14
Std (°)	90	0
Str	0.791	0.334

3.3 Microhardness

To further assess the effect of milling within powder, Vicker’s hardness was measured on the milled surface and across the width of the samples (Fig. 7). A higher load (10 kg) for the Vicker’s hardness testing was employed on the machined surface (XZ plane) to minimize the influence of feed marks. On the cross-sectioned face (YZ plane), samples were polished before indenting using a 1 kg load. Results indicated that milling within powder resulted in a harder surface. Initially, this was thought to be caused by the changes in the tool-workpiece interface that resulted in a burnishing effect by the powder particles that acted to harden the surface. However, after examining the cross-sectioned surface, it seems that milling within powder seemed relatively stable since the surface integrity on the cross-section was unaffected by milling. This means that the cutting process in powder and changes to the tool-workpiece interface had little to no effect on the hardness. The surface that was milled without powder exhibited a more substantial difference in microhardness between the milled and cross-sectioned surfaces. This result suggests that milling without powder likely softens the surface since the cross section is relatively unaffected by machining. It is not clear at this point what the mechanism is behind this decrease. Perhaps it is driven by thermally induced metallurgical changes or residual stress.

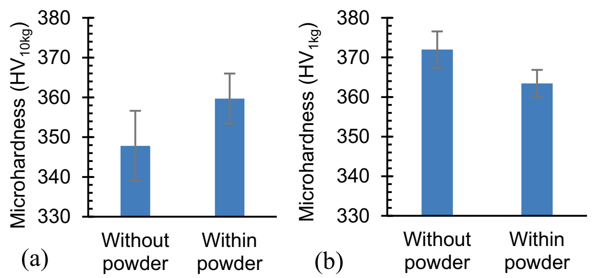

Fig. 7 Microhardness after milling within powder and without powder on (a) the externally milled surface and (b) the cross-sectioned surface that should be unaffected by milling (*i.e.*, baseline measurement).

3.4 Tool wear

The tool wear was qualitatively analyzed based on Fig. 8. Although the cutting time was low, tool wear results showed that the in-powder tool presented noticeable scratches on the flank face (Fig. 8c). This was due to the un-melted powder being trapped between the flank face and the workpiece causing more abrasive wear. The size of the flank wear from milling within powder was greater than milling without powder. There was also noticeable discoloration on the tools. The heat affected zone was larger on the tool cutting within powder and exhibited deeper bluer hues on the surface (Fig. 8f). The rake face of the tool cutting without powder exhibited more crater wear (Fig. 8e). Future work will examine longer cutting times across multiple cutting tool geometries.

4. Conclusions

A Matsuura Lumex Avance-25 that combines powder bed fusion with high-speed micro-milling was used to investigate the influence of unmelted powder on the cutting mechanics and resulting surface topography when a milling tool was plunged into powder on a hybrid powder bed fusion system. The presence of unmelted powder surrounding the workpiece affected the tool-workpiece interface and acted as an abrasive particle that that accelerated tool wear. Cutting without powder introduced angular texture on the surface while cutting within powder was more isotropic with an orthogonal texture between the additive layers and the feed marks. The presence of powder resulted in a smoother surface roughness between 1-2 μm and was likely attributed to the powder within the cutting flutes and between the tool and workpiece

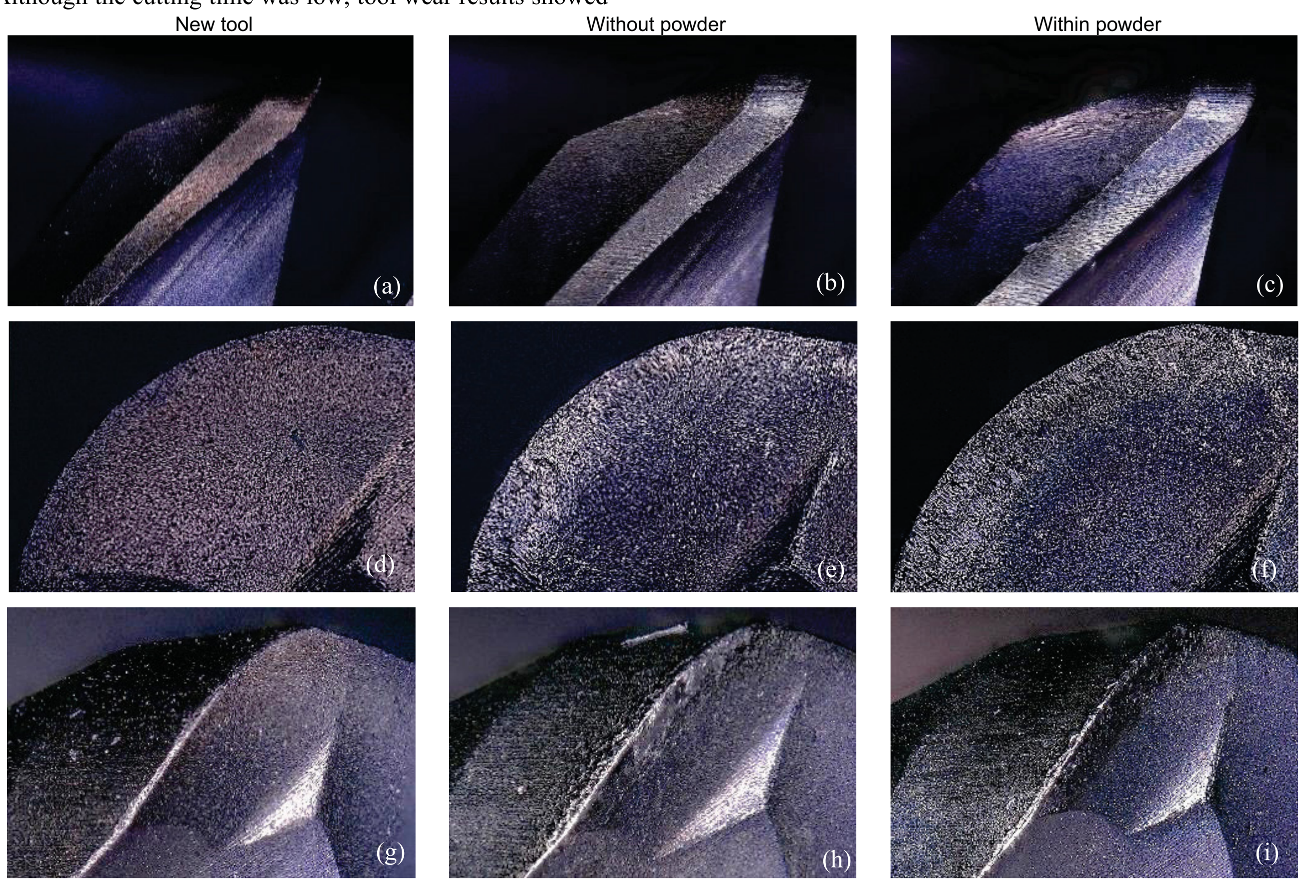

Fig. 8 Tool wear analysis of the flank and rake faces: (a,d,g) new cutting tool; (b,e,h) cutting without powder; (c,f,i) cutting within powder.

interface that resulted in a burnishing effect and/or reduced vibration. It should be noted that surface finishes less than one micron are achievable using finishing cutters within the Lumex; however, this study focused on the most commonly used roughing cutter. Future work will examine the influence of roughing and finishing tools on the surface integrity. The flank wear was higher from cutting in powder while the rake face exhibited more crater wear from cutting without powder.

Acknowledgements

This work was supported in part by the National Science Foundation under award 1953382 as a part of the Research Experiences for Teachers across the National Nanotechnology Coordinated Infrastructure and award 1846478 as a part of CAREER educational activities. Also, the research was performed in part in the Nebraska Engineering Additive Technologies (NEAT) Lab, which is part of the Nebraska Nanoscale Facility supported by the National Science Foundation under Award ECCS: 1542182 and the Nebraska Research Initiative.

References

[1] Sarafan S, Wanjara P, Gholipour J, Bernier F, Osman M, Sikan F, Molavi-Zarandi M, Soost J, Brochu M. Evaluation of maraging steel produced using hybrid additive/subtractive manufacturing. J Manuf Matls Proc. 2021;5(4):107.

[2] Wüst P, Edelmann A, Hellmann R. Areal surface roughness optimization of maraging steel parts produced by hybrid additive manufacturing. Materials. 2020;13(2):418.

[3] Abe S, Higashi Y, Fuwa I, Yoshida N, Yoneyama T. Milling-combined laser metal sintering system and production of injection molds with sophisticated functions. InTowards Synthesis of Micro-/Nano-systems 2007 (pp. 285-290). Springer, London.

[4] Yassin A, Ueda T, Hosokawa A, Furumoto T, Tanaka R, Abe S. Study on cutting characteristics of sintered material with Yb: Fiber laser. J Adv Mech Des Sys Manuf. 2008;2(5):833-843.

[5] Yassin A, Ueda T, Furumoto T, Hosokawa A, Tanaka R, Abe S. Experimental investigation on cutting mechanism of laser sintered material using small ball end mill. J Matls Proc Tech. 2009;209(15-16):5680-5689.

[6] Yassin A, Ueda T, Furumoto T, Aziz MS, Tanaka R, Hosokawa A. Study on tool wear mechanisms in milling laser sintered material. J Mech Sci Tech. 2010;24(1):77-80.

[7] Aziz MS, Ueda T, Furumoto T, Abe S, Hosokawa A, Yassin A. Study on machinability of laser sintered materials fabricated by layered manufacturing system: influence of different hardness of sintered materials. Procedia CIRP. 2012;4:79-83.

[8] Fortunato A, Lulaj A, Melkote S, Liverani E, Ascari A, Umbrello D. Milling of maraging steel components produced by selective laser melting. Intl J Adv Manuf Tech. 2018;94(5):1895-1902.

[9] Breidenstein B, Brenne F, Wu L, Niendorf T, Denkena B. Effect of post-process machining on surface properties of additively manufactured H13 tool steel. HTM J Heat Treatment and Materials. 2018;73(4):173-86.

[10] Leach R. Characterisation of Areal Surface Texture, Springer Science and Business Media. Berlin, Heidelberg; 2013.

[11] Olypus Corporation. Surface Roughness Measurement—Evaluating Parameters. 2021; https://www.olympus-ims.com/en/metrology/surface-roughness-measurement-portal/evaluating-parameters/.

[12] Toh CK. Surface topography analysis in high speed finish milling inclined hardened steel. Precision Engineering. 2004;28(4):386-398.

[13] Kang MC, Kim KK, Lee DW, Kim JS, Kim NK. Characteristics of inclined planes according to the variations of cutting direction in high-speed ball-end milling. Intl J Adv Manuf Tech. 2001;17(5):323-329.